

**Liquid ammoniates as efficient electrolytes for room-temperature rechargeable sodium metal batteries based on an organic cathode**

•

Débora Ruiz-Martínez, Teresa Lana-Villarreal, Roberto Gómez\*

*Departament de Química Física i Institut Universitari d'Electroquímica, Universitat d'Alacant,*

*Apartat 99, E-03080 Alacant, Spain.*

\*Corresponding author: Roberto.Gomez@ua.es

**CONTENT**

1. FESEM micrograph for PAQS particles	S2
2. Potential window for PAQS electrodes	S2
3. Electrochemical behavior optimization for PAQS electrodes	S3
4. Cyclic voltammogram evolution as a function of the number of charge-discharge cycles	S9
5. Aspect of the split cell elements after electrochemical cycling	S10
6. Chemical reduction of PAQS	S11
7. SEM images for a PAQS electrode before and after 300 charge-discharge cycles	S12
8. REFERENCES	S13

**1. FESEM image for PAQS particles powder.**

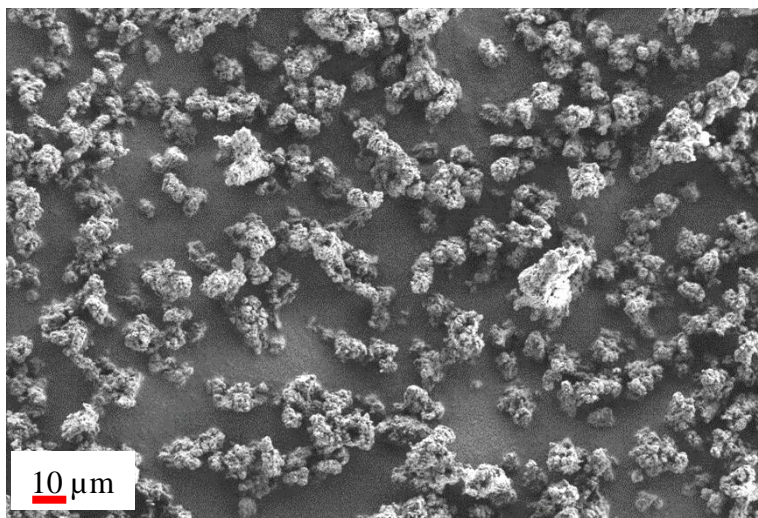


**Figure S1.** FESEM for PAQS particles powder. As observed, the PAQS particles possess a quasi spherical shape with a diameter in between 3 and 10  $\mu\text{m}$ .

**2. Potential window for PAQS electrodes**

Figure S2 shows cyclic voltammograms for a PAQS electrode in  $\text{NaI} \cdot 3.3\text{NH}_3$  employing different electrode potential windows. The positive potential limit was fixed at 2.6 V vs.  $\text{Na}^+/\text{Na}$  due to the electrolyte oxidation, while the negative potential limit was sequentially modified from 1.2 V (black) to 0.2 V (red). When the limit was set at potentials more negative than 1.2 V vs.  $\text{Na}^+/\text{Na}$ , an irreversible reduction current appears which still can be observed in the third scan. Besides, the characteristic voltammetric peaks of PAQS were also affected becoming ill-defined. These results suggest an irreversible reduction of PAQS at potentials more negative than 1.2 V vs.  $\text{Na}^+/\text{Na}$ , which can be ascribed to the rupture of S-S bonds.

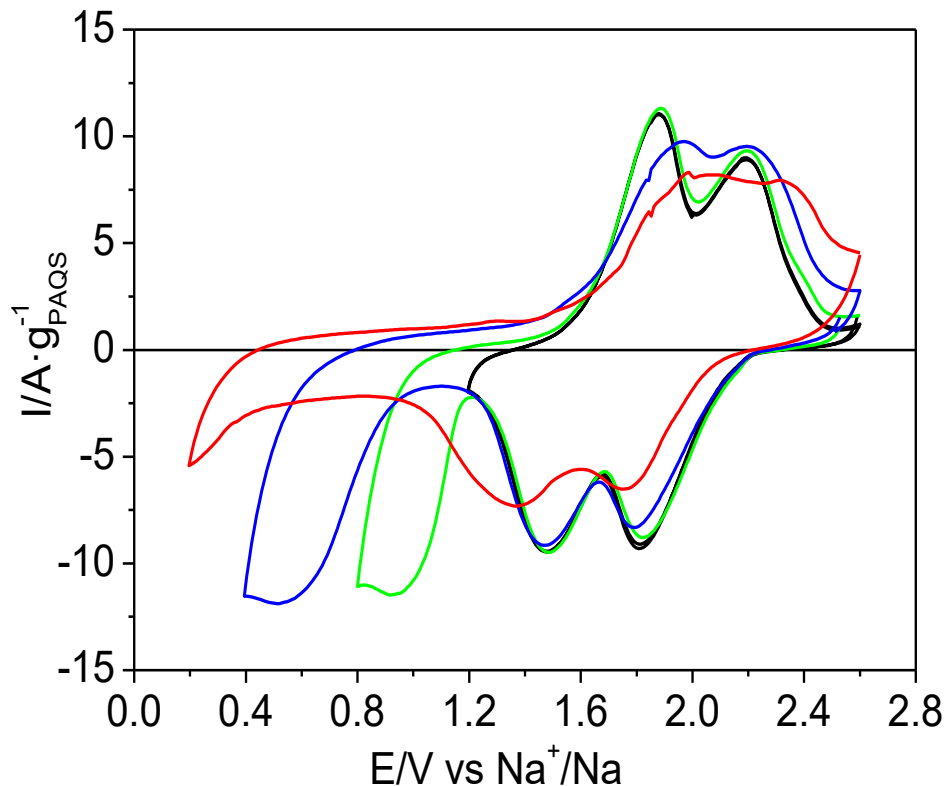


**Figure S2.** Cyclic voltammograms recorded at  $20 \text{ mV} \cdot \text{s}^{-1}$  for a PAQS electrode in  $\text{NaI} \cdot 3.3\text{NH}_3$ , varying sequentially the negative potential limit to 1.2 V (black), 0.8 V (green), 0.4 V (blue) and 0.2 V (red). The experiments were carried out at room temperature in a two-electrode split cell using sodium metal as an anode.

### 3. Electrochemical behavior optimization for PAQS electrodes

- Optimization of PAQS electrode composition and pressure applied during the preparation procedure.

To improve the PAQS electrochemical behavior, carbon nanotubes (NTs) were used as a conductive additive while PTFE was used as a binder. Different electrode compositions were tested. All the electrodes were prepared by the *dry-pressing technique* employing  $4 \text{ mg} \cdot \text{cm}^{-2}$  as mass loading and different applied pressures.

The pressure applied on the electrodes impacts directly on its electrochemical behavior. If the pressure is too low, the electrode is usually mechanically unstable, as the polymer particles can be detached from the conducting substrate. On the other hand, if the pressure is too high, the porosity of the electrode notably diminishes and, thus, the real interfacial area, affecting the final electrochemical behavior. Table S1 shows a summary of the different compositions and applied pressures tested. The symbol ✓ indicates that the pressure applied enables an adequate electrochemical behavior, while the symbol ✗ indicates that the electrode behavior is poor. According to the data collected, the optimum pressure for a 4 mg·cm<sup>-2</sup> PAQS electrode is around a value of 1.5 ton·cm<sup>-2</sup> applied for 2 min.

**Table S1.** Composition of PAQS electrodes and effect of the pressure applied during preparation.

Composition for PAQS electrode/ wt%				Pressure applied for 2 minutes/ ton·cm <sup>-2</sup>			
Number	PAQS	NTs	PTFE	0.5	1	1.5	2
(1)	40	50	10	✓	✓	✓	✗
(2)	50	40	10	✗	✓	✓	✗
(3)	60	30	10	✗	✓	✓	✗
(4)	80	10	10	✗	✗	✗	✓

Figure S3 shows the stationary cyclic voltammogram (usually the third cycle) for PAQS electrodes with the different compositions shown in Table S1 at  $5 \text{ mV} \cdot \text{s}^{-1}$  in  $\text{NaI} \cdot 3.3\text{NH}_3$  using the optimized pressure of  $1.5 \text{ ton} \cdot \text{cm}^{-2}$  for 2 min. As observed, the electrochemical behavior strongly depends on the PAQS:NTs:PTFE ratio (value specified between parentheses). Electrodes (2) (50:40:10) and (3) (60:30:10) show larger specific currents in comparison with electrodes (1) (40:50:10) and (4) (80:10:10). As there are no significant differences in the electrochemical behavior of electrodes (2) and (3), the composition of electrode (3) with PAQS:NTs:PTFE in proportions 60:30:10 was chosen as the optimum one. It contains a ratio of NTs smaller than that of (2) and thus, it could be more cost-effective in a future application.

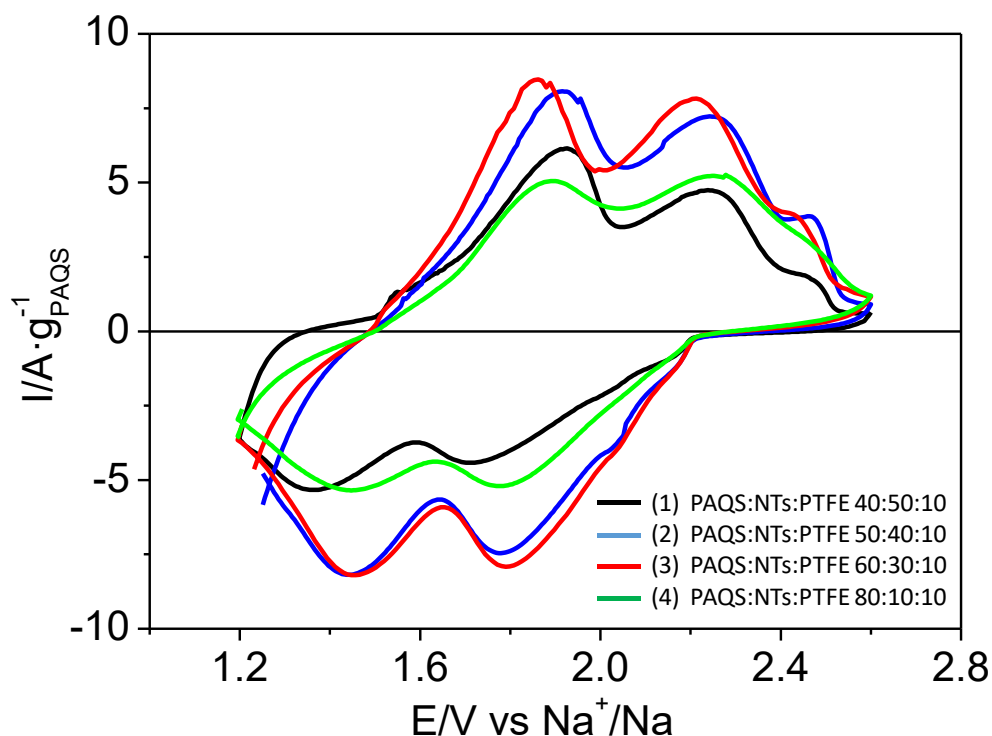


**Figure S3.** Cyclic voltammograms at  $5 \text{ mV} \cdot \text{s}^{-1}$  for several PAQS electrode compositions in  $\text{NaI} \cdot 3.3\text{NH}_3$ . The experiments were performed at room temperature in a two-electrode split cell using sodium metal as an anode.

➤ Study of the effect of the additive nature on the electrochemical behavior

The effect of the conductive additive and binder nature on the electrochemical behavior was also studied. The electrodes were prepared by the *dry-pressing* technique with a mass loading of 4

mg·cm<sup>-2</sup>. Table S2 shows a summary of the electrodes tested. Carbon Super P (C Super P, from Timcal Graphite&Carbon, Super P Conductive carbon black, 80g/bag) was selected as an alternative to carbon NTs while PVDF was studied as a binder alternative to PTFE.

**Table S2.** PAQS electrode optimization: additive nature.

Composition of PAQS electrode/ wt%					
Number	PAQS	NTs	C Super P	PTFE	PVDF
(1')	60	30	0	10	0
(2')	60	0	30	10	0
(3')	67	33	0	0	0
(4')	60	30	0	0	10

Figure S4 shows the cyclic voltammograms at 5 mV·s<sup>-1</sup> for the different PAQS compositions shown in Table S2 in NaI·3.3NH<sub>3</sub>. As observed, electrodes **(1')** (PAQS:NTs:PTFE 60:30:10) and **(2')** (PAQS:CSuperP:PTFE 60:30:10) show higher current densities and better definition of the redox processes than electrode **(3')** (PAQS:NTs 67:33) and **(4')** (PAQS:NTs:PVDF 60:30:10). The advantage of using carbon NTs in the formulation comes from the fact that they provide higher specific capacity than carbon Super P. In addition, carbon NTs combine such a high specific area with an elongated morphology that facilitates the electron transport between the PAQS particles and the conducting substrate which is not the case of carbon Super P due to its spherical geometry.<sup>1,2</sup>

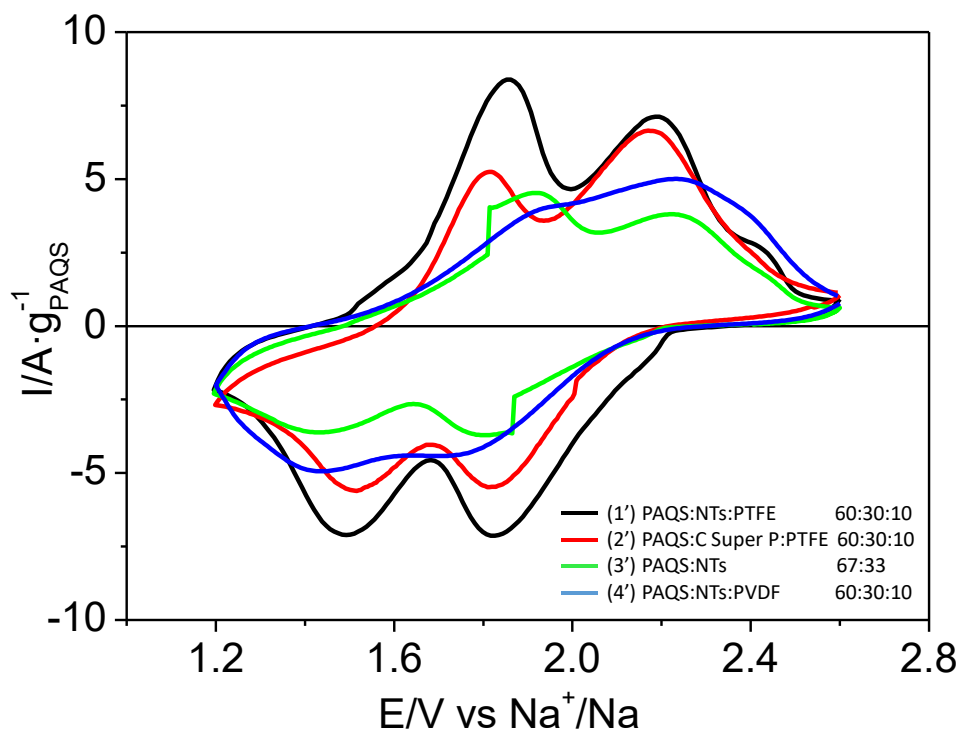


**Figure S4.** Cyclic voltammograms at  $5 \text{ mV} \cdot \text{s}^{-1}$  in  $\text{NaI} \cdot 3.3\text{NH}_3$  for several electrode compositions. The experiments were performed at room temperature in a two-electrode split cell using sodium metal as an anode.

➤ Effect of the mass loading on the electrochemical behavior of the electrodes

PAQS electrodes (PAQS:NTs:PTFE in proportions 60:30:10) with different mass loadings of 4 mg, 8 mg and 16 mg were prepared (on a geometrical area of  $1 \text{ cm}^2$ ). Figure S5 shows the cyclic voltammograms recorded at  $5 \text{ mV} \cdot \text{s}^{-1}$  in  $\text{NaI} \cdot 3.3\text{NH}_3$ . As observed, the gravimetric capacity linearly decreases with the mass loading. In addition, the redox processes of PAQS become less defined. Generally, thicker electrodes show a worse electrochemical behavior than thinner ones and present limitations of ion and electron transport.<sup>3</sup> These features could be exacerbated by the *dry-pressing* technique used to prepare the PAQS electrode.

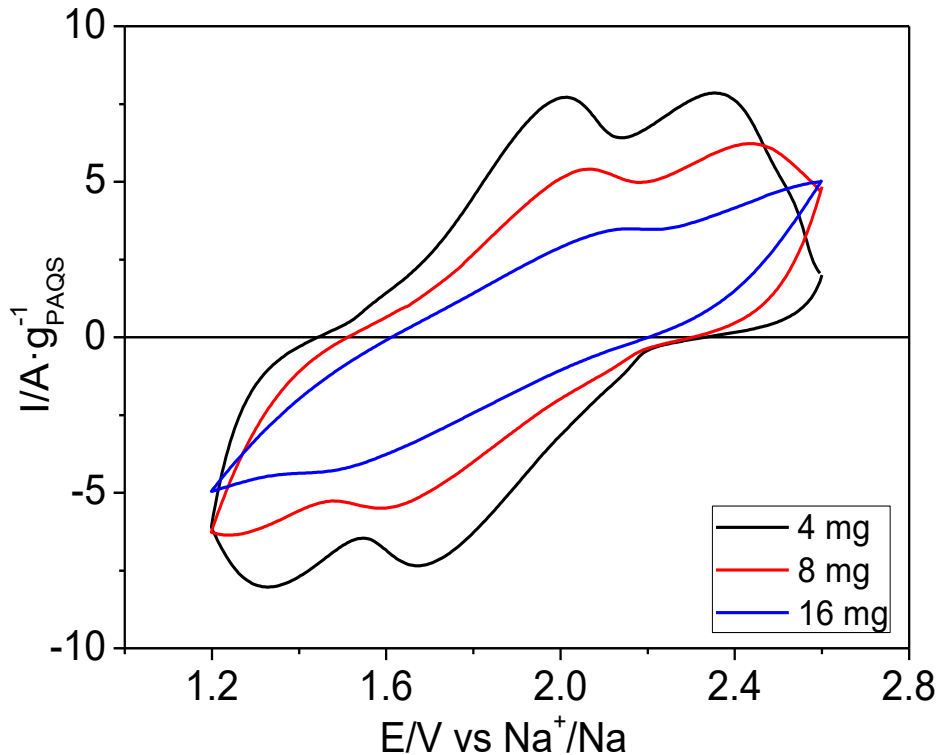


**Figure S5.** Cyclic voltammograms at 5 mV·s<sup>-1</sup> in NaI·3.3NH<sub>3</sub> for electrodes (1 cm<sup>2</sup>) with different mass loadings: 4 mg (black), 8 mg (red) and 16 mg (blue). The experiments were performed at room temperature in a two-electrode split cell using sodium metal as an anode.

➤ Mechanical treatment of PAQS particles in the ball mill.

Two different procedures have been employed for ball milling, depending on whether only PAQS particles are mechanically treated, or all cathode components are mixed. The ball milling technique is typically employed to diminish the particle size, to promote both a homogeneous mixture among the different electrode components (active material, conducting carbon, and binder) and the contact or interaction among them. Parameters as the spin rate or time directly affect the particle size and the mixture homogeneity. In the case of PAQS, a mild procedure (100 rpm and 3 h) was chosen due to its polymeric nature. The best results regarding particle size were obtained under the conditions mentioned above. Otherwise, PAQS particles tend to agglomerate and stick together. When carbon nanotubes were introduced into the mixture, increasing the spin rate of the ball mill treatment was shown to be appropriate, enabling the use of shorter times (350rpm and 1h). Carbon nanotubes



mixed with the PAQS particles avoid their agglomeration during the mechanical treatment. In addition, smaller PAQS particles can be obtained, mainly due to the higher spin rates.

#### 4. Cyclic voltammogram evolution as a function of the number of charge-discharge cycles

Figure S6 shows the evolution of the cyclic voltammogram for a PAQS electrode during 300 charge-discharge cycles. The shape of the voltammogram significantly changes from the initial cycle (black) to cycle 300 (red). The average current density decreases and the definition of the redox processes of PAQS is lost during the electrochemical cycling.

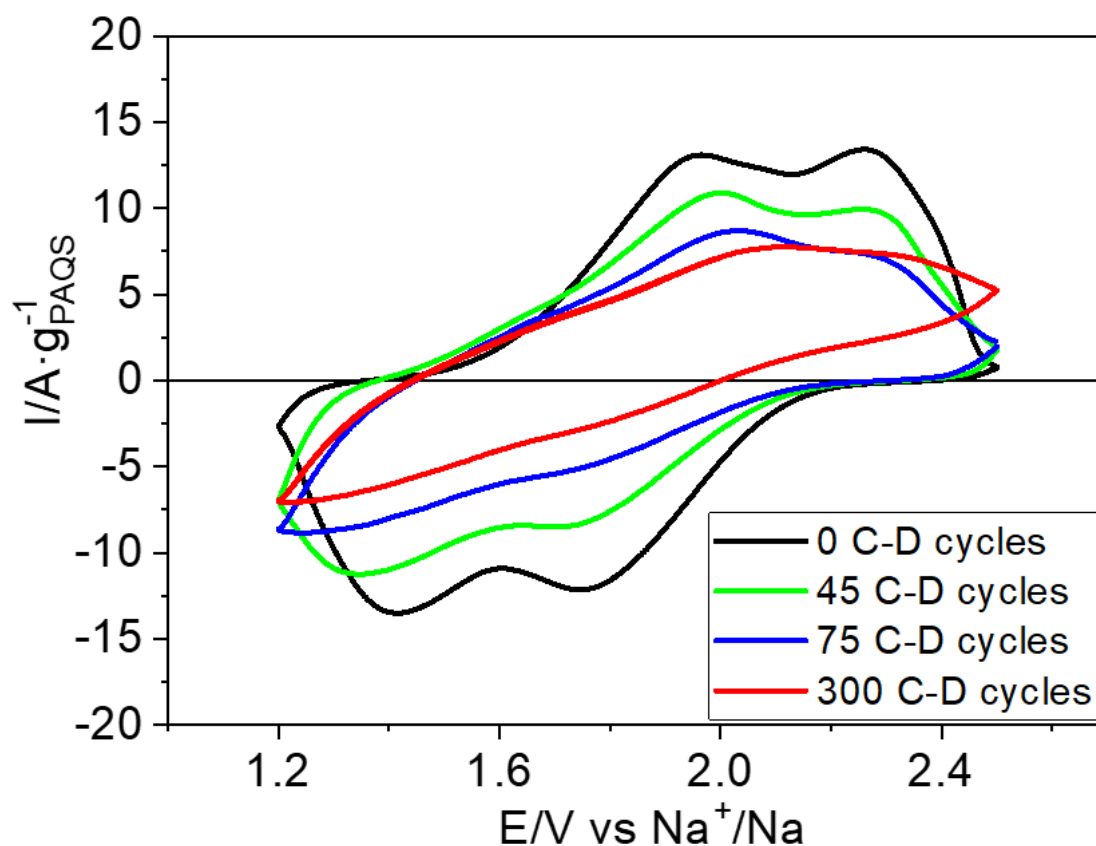


**Figure S6.** Evolution of the cyclic voltammograms as a function of the charge-discharge (C-D) cycles for a PAQS electrode in NaI·3.3NH<sub>3</sub>. The cyclic voltammograms were recorded at room temperature at 20 mV·s<sup>-1</sup> in a two-electrode split cell using sodium metal as an anode.

### 5. Aspect of the split cell elements after electrochemical cycling

Figure S7 shows the appearance of the split cell elements after electrochemical cycling. The image shows: the Whatman separator paper, the PAQS electrode surface and the sodium electrode after 300 charge-discharge cycles. The yellowish-orange coloration of the separator paper can be related to the presence of reduced PAQS. A slight coloration on the sodium surface is also observed, pointing to the cross-over of reduced PAQS through the separator.

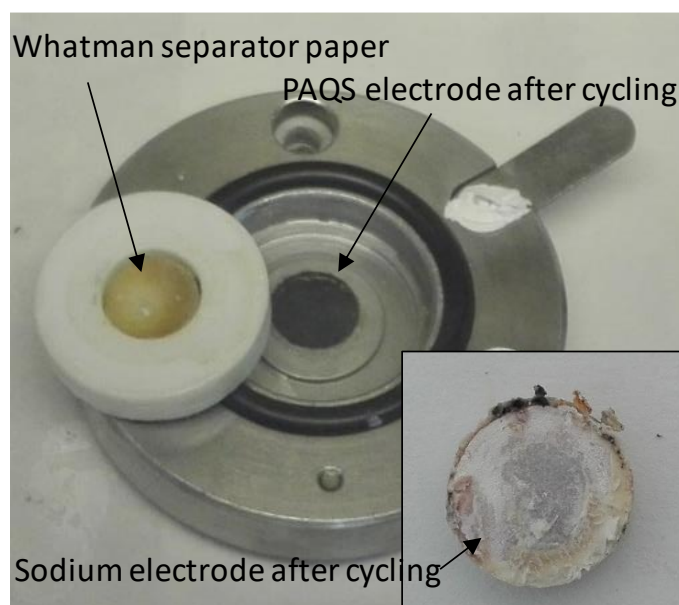


**Figure S7.** Aspect of the split cell after electrochemical cycling.

## 6. Chemical reduction of PAQS

A PAQS electrode was chemically reduced using  $\text{NaBH}_4$  as a reducing agent. The PAQS electrode was introduced in a solution containing 0.1 M NaOH in methanol and 0.2 M  $\text{NaBH}_4$ . Immediately after immersion, an orange-red coloration appeared in the solution, which became increasingly darker (Figure S8 (a) to (c)). This experiment is a clear indication that reduced PAQS is highly soluble in polar solvents.

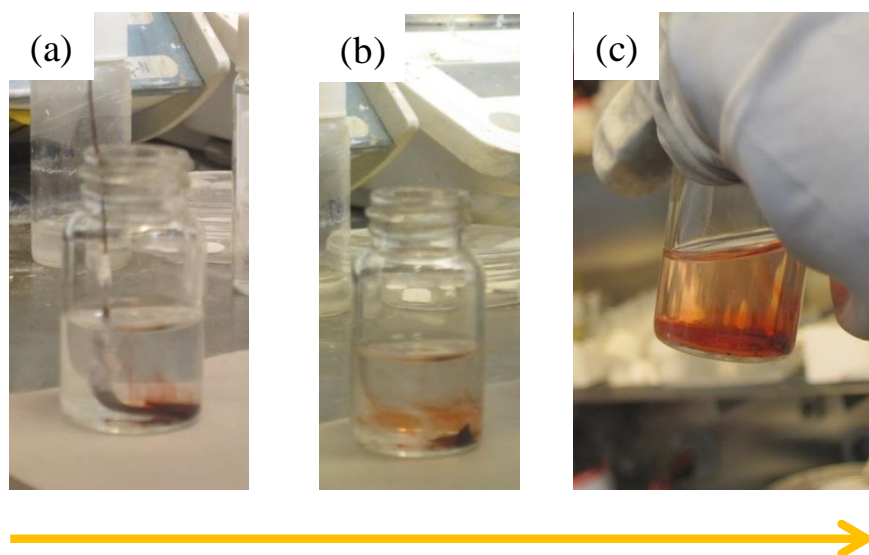


**Figure S8.** Chemical reduction of PAQS in a solution containing 0.1 M NaOH in methanol and 0.2 M  $\text{NaBH}_4$ . Images (a) to (c) show the color evolution after the PAQS electrode immersion.

## 7. SEM images for a PAQS electrode before and after 300 charge-discharge cycles

Figure S9(b) shows a SEM image for the PAQS electrode after 300 charge-discharge cycles. For comparison an image of the electrode surface prior to the electrochemical experiments is also included (Figure S9(a)). Significant morphological changes occur during the electrochemical cycling. For example, the naked carbon NTs are no longer observed, pointing to the dissolution of PAQS during its electrochemical reduction, and its redeposition process on the NTs during the subsequent oxidation process. In agreement, the particle edges become ill-defined.

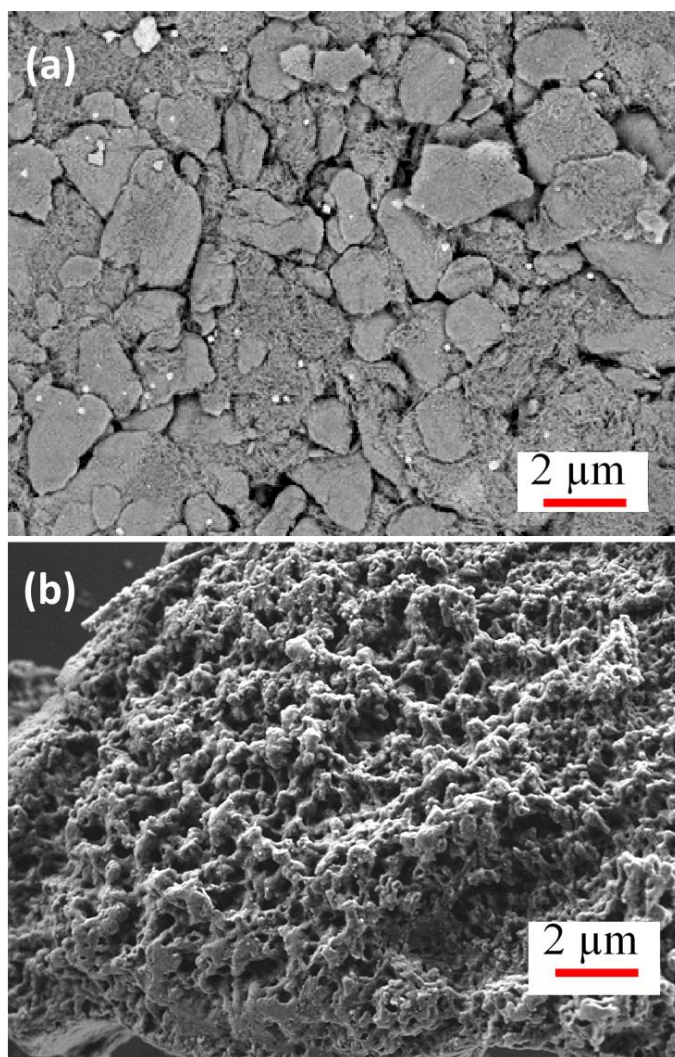


**Figure S9.** SEM image for PAQS electrodes before (a) and after (b) 300 charge-discharge cycles.

## **REFERENCES**

- [1] Zheng, X.; Dong, C.; Huang, B.; Lu, M. Effects of Conductive Carbon on the Electrochemical Performances of  $\text{Li}_4\text{Ti}_5\text{O}_{12}/\text{C}$  Composites, *Int. J. Electrochem. Sci.* **2012**, 7, 9869–9880.
- [2] George, C.; Morris, A.J.; Modarres, M.H.; De Volder, M. Structural Evolution of Electrochemically Lithiated  $\text{MoS}_2$  Nanosheets and the Role of Carbon Additive in Li-Ion Batteries, *Chem. Mater.* **2016**, 28, 7304–7310. <https://doi.org/10.1021/acs.chemmater.6b02607>.
- [3] Huang, X.; Ke, S.; Lv, H.; Liu, Y. A dynamic capacity fading model with thermal evolution considering variable electrode thickness for lithium-ion batteries, *Ionics*, **2018**, 24, 3439–3450, <https://doi.org/10.1007/s11581-018-2476-8>.